Computer-Aided Diagnosis and Tuning of Cascaded Coupled Resonators Filters

Heng-Tung Hsu, *Student Member, IEEE*, Hui-Wen Yao, *Senior Member, IEEE*, Kawthar A. Zaki, *Fellow, IEEE*, and Ali E. Atia, *Fellow, IEEE*

***Abstract*—A model for the determination of the individual resonant frequencies and inter-resonator couplings of a system consisting of cascaded coupled resonators is presented. Measuring or computing the phase of the reflection coefficient of short-circuit terminated networks synthesizes all the inter-resonator couplings and resonant frequencies. The loading effect on the last resonator due to the unknown position of the short-circuit reference plane is accurately accounted for by a systematic method. A deterministic finite steps tuning method based on the model is developed. The method is proven successful experimentally and the noniterative nature of the method makes fully automatic tuning of filters possible.**

***Index Terms*—Computer-aided, filters, tuning.**

I. Introduction

THE tuning process for high-performance microwave filters consisting of many resonators is nontrivial, time-consuming, and very expensive [1]–[3]. The main reason is that the element values of the microwave filters, resonators, and coupling elements cannot be measured separately. In many applications, highly accurate couplings and resonant frequencies of individual cavities are necessary to ensure the desired responses of filters. Thus, accurate determination of individual resonant frequencies and inter-resonator couplings of coupled resonators together with a deterministic tuning algorithm are essential for minimizing the tuning effort.

The conventional methods of tuning filters, based on the process described by Dishal [1], utilize the filter return loss as the criterion for tuning. The person tuning the filter basically minimizes the reflection coefficient of the doubly terminated filter in its passband by adjusting tuning screws until an acceptable response is obtained. This is an empirical time-consuming process. The main difficulty is that each tuning screw affects the whole response of the filter and there is no direct correlation between the change of a tuning screw and the resulting change in filter response. A method for measurement of inter-resonator couplings introduced by Atia and Williams [2] is based on measuring the phase responses of the reflection coefficient of a short-circuited network consisting of identical and synchronously tuned coupled resonators. This method has been widely used for tuning of various microwave filters and multiplexers [4], [5]. However, the method requires successive trials to achieve synchronous tuning of all resonators to the same resonant frequency, which is a tedious iterative and qualitative process. Successive synchronous tuning of all resonators may be difficult due to lack of direct access to each individual resonator. Furthermore, the methods in [1] and [2] cannot be adequate for filters that have resonators with different resonant frequencies [6].

Thal [3] developed a method that incorporated equivalent-circuit analysis programs with element-optimization routines. Basically, the method starts from an initial measurement of the filter response followed by the generation of a circuit model obtained from optimizing the circuit elements to fit the measured response. Filter alignment and diagnosis are performed through the optimized circuit model. The whole process is repeated iteratively until acceptable responses are achieved. Phase method of diagnostics and tuning has been widely used for filter tuning [7], [8]. Accatino [7] utilized phase measurement of the input admittance of a short-circuited filter in conjunction with LCX synthesis and minimum pattern search optimization techniques to extract inter-cavity couplings and resonant frequencies of individual cavities. Among all the previously proposed approaches, the iterative characteristics make the tuning process a tedious job. Until now, the tuning of filters has been as much art as science. The main difficulties are the lack of a deterministic tuning algorithm and the direct correlation between the measured parameters and the resulting filter responses. Another method, such as the time-domain tuning method, which utilized the discrete inverse Fourier transform to get the time-domain response, has also been presented [9].

In this paper, a comprehensive equivalent-circuit model is proposed to determine the inter-resonator couplings and the individual resonant frequencies of cascaded coupled-resonator filters. Closed-form recursive formulas are presented, which calculate couplings and resonant frequencies from the zeros and poles of the input impedance of cascaded resonators with a short circuit at one port. The importance of the loading effect, caused by the unavoidable unknown shift in the short-circuit reference plane, is addressed and effectively removed by a systematic method. While the model provides a direct correlation between the measured parameters (zeros and poles) and the resulting filter response, a deterministic tuning method in a finite known number of tuning steps is also developed to eliminate the tedious iterative process required in other tuning methods. In general, only $(2n-1)$ tuning steps are necessary for a filter with n resonators. The proposed method also finds its application in conjunction with full-wave simulations to simulate and compute the

Manuscript received January 13, 2001.

H.-T. Hsu and K. A. Zaki are with the Department of Electrical and Computer Engineering, University of Maryland at College Park, College Park, MD 20742 USA.

H.-W. Yao and A. E. Atia are with the Orbital Sciences Corporation, Germantown, MD 20874 USA.

Publisher Item Identifier S 0018-9480(02)03019-3.

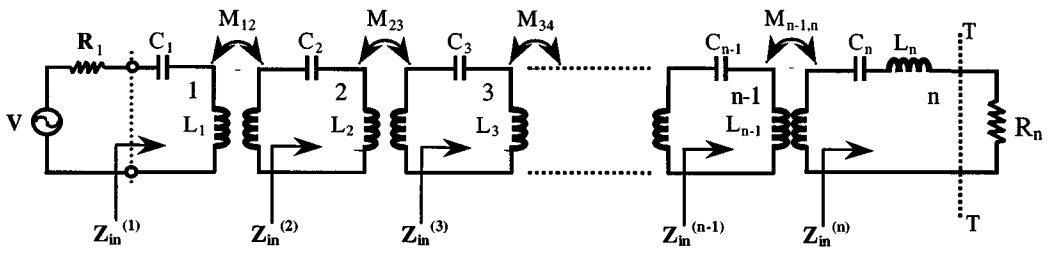

Fig. 1. Equivalent-circuit representation for the cascaded coupled resonators filter.

inter-resonator couplings and resonant frequencies of coupled nonidentical cavities [10]. Although only the cascaded coupled resonators filters are considered, the process can also be effectively applied in tuning and diagnosis of coupled resonators filters with cross couplings. This is the case since, in practice, the cross couplings are usually small and one can always select the tuning path involving only the cascaded resonators. The application of the method to the tuning of a five-pole combline Chebyshev filter is also presented. The promising results showed the powerfulness of the method and implied the feasibility of full automation in filter tuning.

II. Circuit Model of Cascaded Coupled Resonators

Fig. 1 shows the equivalent circuit of a two-port lumped-element network consisting of n cascaded coupled resonators. Each resonator is composed of a series capacitance C_i, $i = 1,\ldots,n$ together with total loop inductance L_i and is characterized by its individual resonant frequency $\omega_{oi} = \sqrt{1/L_iC_i}$ and characteristic impedance $Z_{oi} = \sqrt{L_i/C_i}$. Couplings between the adjacent resonators are represented by the frequency independent reactances $M_{i,i+1}$, while R_1 and R_n are the equivalent resistances representing the input (source) and output (load) couplings, respectively. Although this network model is valid for narrow bandwidth, it is usually sufficient in most of the applications. When resonator n in Fig. 1 is terminated in a short circuit at the reference plane T–T, the input impedance at loop i can be derived as

$$Z_{\text{in}}^{(i)} = j\frac{Z_{oi}}{\omega\omega_{oi}}\frac{P_i(\omega^2)}{Q_i(\omega^2)}, \qquad i = 1,\ldots,n \tag{1}$$

where $P_i(\omega^2)$ and $Q_i(\omega^2)$ are monic polynomials of orders $(n-i+1)$ and $(n-i)$; Z_{oi} and ω_{oi} are the characteristic impedance and resonant frequency of resonator i.

For the network shown in Fig. 1, $P_i(\omega^2)$ and $Q_i(\omega^2)$ can be expressed as [11], [12]

$$\begin{aligned} P_i(\omega^2) &= \sum_{t=0}^{n-i+1} c_t^{(i)}(\omega^2)^t \\ &= \prod_{t=1}^{n-i+1}\left(\omega^2 - \omega_{zt}^{(i)^2}\right), \qquad i = 1,2,\ldots,n \end{aligned} \tag{2}$$

$$\begin{aligned} Q_i(\omega^2) &= \sum_{q=0}^{n-i} d_q^{(i)}(\omega^2)^q \\ &= \prod_{q=1}^{n-i}\left(\omega^2 - \omega_{pq}^{(i)^2}\right), \qquad i = 1,2,\ldots,n \end{aligned} \tag{3}$$

where $\omega_{zt}^{(i)^2}$ $(t = 1,2,\ldots,n-i+1)$ and $\omega_{pq}^{(i)^2}$ $(q = 1,2,\ldots,n-i)$ are the zeros of $P_i(\omega^2)$ and $Q_i(\omega^2)$, corresponding to the zeros and poles of the input impedance of the one port network at loop i, respectively.

The coupling coefficient $(k_{i,i+1})$ between two adjacent resonators is related to the frequency independent reactances $M_{i,i+1}$ as

$$k_{i,i+1}^2 = \frac{M_{i,i+1}^2}{Z_{oi}Z_{oi+1}}, \qquad i = 1,2,\ldots,n-1. \tag{4}$$

Analysis of the short-circuited one-port network yields the following simple closed-form recursive relations [13]

$$P_{i+1}(\omega^2) = Q_i(\omega^2), \qquad i = 1,2,\ldots,n-1 \tag{5}$$

$$m_{i,i+1}^2\omega^2 Q_{i+1}(\omega^2) = \left(\omega^2 - \omega_{0i}^2\right)P_{i+1}(\omega^2) - P_i(\omega^2), \qquad i = 1,2,\ldots,n-1. \tag{6}$$

with

$$\begin{aligned} \omega_{0i}^2 &= \frac{\prod_{t=1}^{n-i+1}\omega_{zt}^{(i)^2}}{\prod_{q=1}^{n-i}\omega_{pq}^{(i)^2}} \\ &= -\frac{c_0^{(i)}}{d_0^{(i)}}, \qquad i = 1,2,\ldots,n \end{aligned} \tag{7}$$

$$\begin{aligned} m_{i,i+1}^2 &= \omega_{0i}\omega_{0,i+1}\frac{M_{i,i+1}^2}{Z_{0i}Z_{0,i+1}} \\ &= \omega_{0i}\omega_{0,i+1}k_{i,i+1}^2 \\ &= \sum_{t=1}^{n-i+1}\omega_{zt}^{(i)^2} - \sum_{q=1}^{n-1}\omega_{pq}^{(i)^2} - \omega_{0i}^2 \\ &= d_{n-i-1}^{(i)} - c_{n-i}^{(i)} - \omega_{0i}^2, \qquad i = 1,2,\ldots,n-1. \end{aligned} \tag{8}$$

In the above equations, $m_{i,i+1}$ is defined as the coupling bandwidth, equivalent to the coupling coefficient in frequency units. The above recursive relations provide a simple and direct correlation between the filter parameters (the inter-resonator couplings and the resonant frequencies of individual resonators) and the zeros and poles of the input impedance of the short-circuited network, though we do not have direct access to each individual resonator in the filter.

The zeros and poles of the short-circuited network can be obtained either by direct measurement or by numerical simulation. In the case of direct measurement, where the reference plane is clearly defined, the frequencies corresponding to $\pm 180^\circ$ and 0° phases are the corresponding zeros and poles of the input impedance. In some situations, linear interpolation technique might be necessary to determine such frequencies, depending on the setup of test instruments. As for the case of numerical simu-

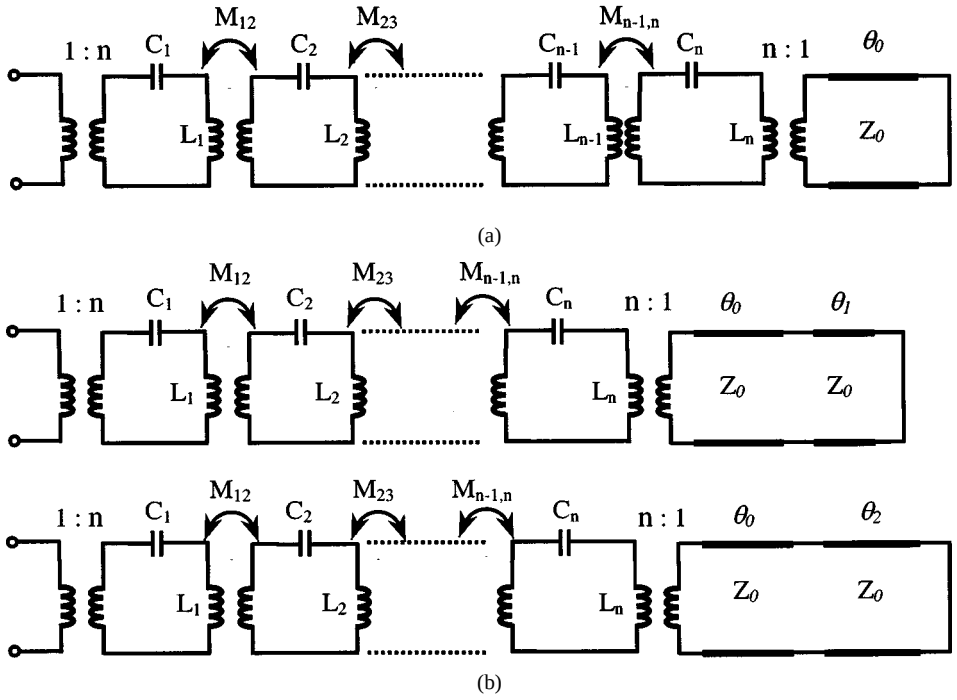

Fig. 2. (a) Modified equivalent-circuit model with an extra piece of transmission line to account for the shift in the short-circuit reference plane. (b) Two different setups for the additional two measurements to remove the loading effect to the last resonator by the proposed method.

lation, however, the locations of the zeros and poles can be determined through the calculation of phase derivatives with respect to frequency. Those frequencies at which the phase derivative evaluated is the maximum (minimum) are the corresponding zeros (poles) of the input impedance. Finally, the input (output) coupling resistance r_1 (r_n) in frequency unit is also related to the zeros and poles through the following equation:

$$r_{1,n} = \left| \frac{\prod_{i=1}^{n} \left(\omega_R^2 - \omega_{zi}^{(1)^2} \right)}{\omega_R \prod_{q=1}^{n-1} \left(\omega_R^2 - \omega_{pq}^{(1)^2} \right)} \right| \tag{9}$$

where ω_R is the frequency corresponding to $\pm 90^\circ$ phase of the input reflection coefficient.

III. Removal of Loading Effect

From Section II, it is clear that all the inter-resonator couplings and resonant frequencies of the individual resonators can be extracted through the proposed model once the zeros and poles of the input impedance are known. Hence, highly accurate determination of zeros and poles of the input impedance is essential to guarantee the exact diagnosis and tuning of the filter. Basically, all the derivations in Section II are based on the one-port network with a short-circuited termination directly at the end of the last resonator. However, in practice, this is not possible due to the lack of direct access to the last resonator inside the filter. An unknown length of additional transmission line is unavoidable between the output coupling structure and the short-circuit reference plane, which results in additional loading to the last resonator.

Consider the modified equivalent-circuit representation, as shown in Fig. 2(a). An additional piece of transmission line with unknown length θ_o is added between the output coupling structure (represented as a transformer with turns ratio $n = \sqrt{Z_o/R_n}$) and the short-circuit termination to account for the shift in reference plane. The input impedance of the last resonator of this modified network can be obtained as

$$Z_{\text{in}} = -j \frac{M_{n-1,n}^2}{Z_{\text{on}} \lambda + \left(\frac{Z_o}{n^2} \right) \tan \theta_o}$$
$$\lambda = \frac{f}{f_{\text{on}}} - \frac{f_{\text{on}}}{f} \tag{10}$$

where Z_{on} and f_{on} are the characteristic impedance and the resonant frequency of the last resonator; Z_o is the characteristic impedance of the additional transmission line (usually 50 Ω). The following relationship holds at the measured natural frequency $f_{\text{on}}^{(1)}$ of the structure

$$\lambda_1 \equiv \frac{f_{\text{on}}^{(1)}}{f_{\text{on}}} - \frac{f_{\text{on}}}{f_{\text{on}}^{(1)}} = -\frac{R_n}{Z_{\text{on}}} \tan \theta_0 \tag{11}$$

while $f_{\text{on}}^{(1)}$ is extracted from the measured zeros and poles of the short-circuited network, the remaining three unknowns in the above equation are θ_o, f_{on}, and Z_{on}. To obtain enough information for solving θ_o, two additional measurements are made by inserting two different transmission lines with known length θ_1 and θ_2, as shown in Fig. 2(b). At the measured natural frequencies $f_{\text{on}}^{(2)}$ and $f_{\text{on}}^{(3)}$ of the two different setups, we have

$$\lambda_2 \equiv \frac{f_{\text{on}}^{(2)}}{f_{\text{on}}} - \frac{f_{\text{on}}}{f_{\text{on}}^{(2)}} = -\frac{R_n}{Z_{\text{on}}} \tan(\theta_o + \theta_1) \tag{12}$$

$$\lambda_3 \equiv \frac{f_{\text{on}}^{(3)}}{f_{\text{on}}} - \frac{f_{\text{on}}}{f_{\text{on}}^{(3)}} = -\frac{R_n}{Z_{\text{on}}} \tan(\theta_o + \theta_2). \tag{13}$$

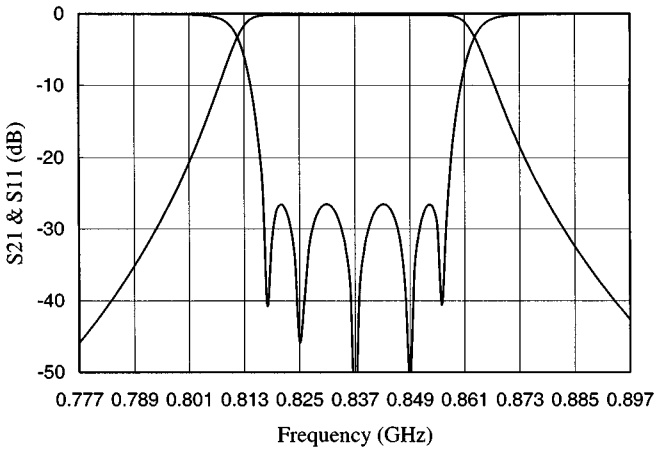

Fig. 3. Theoretical response of the five-pole combline Chebyshev filter with center frequency of 836.5 MHz and bandwidth of 40 MHz.

It should be clear that certain relationship exists for the "unperturbed" resonant frequency of the last resonator $f_{\rm on}$ and those "perturbed" ones, i.e., $f_{\rm on}^{(1,2,3)}$, as

$$f_{\rm on} > f_{\rm on}^{(1)} > f_{\rm on}^{(2,3)}. \tag{14}$$

Equations (11)–(13) can be used to solve for all the unknowns, particularly the length θ_0, which accounts for the shift in the short-circuit reference plane. The appropriate solution will be the one that satisfies the constraint outlined in (14).

Despite the simplicity of the proposed method for solving θ_0, the choices of the length of θ_1 and θ_2 should be carefully addressed. Theoretically, the perturbations (the length of θ_1 and θ_2) must be small enough so that the networks remain under the condition of being near the optimum approximation for (2) and (3) to be valid. This is equivalent to that fact that, in practical situations, θ_1 and θ_2 should be so short that the existence of all the zeros and poles of the phase of input reflection coefficient is guaranteed on the display of the test instrument (vector network analyzer). Once θ_0 is known, the same analysis procedure, as discussed in Section II, is performed on the modified equivalent-circuit representation. It can be easily shown that all the closed-form recursive relations [see (5)–(8)] remain unchanged. The only parameter necessary to be adjusted is the resonant frequency of the last resonator. For a given θ_0, the difference between the perturbed and unperturbed resonant frequencies of the last resonator can be derived as

$$\Delta f = -\frac{1}{2} \cdot \mathrm{BW} \cdot R_n \cdot \tan\theta_o \tag{15}$$

where BW is the bandwidth of the filter and R_n is the equivalent output coupling resistance.

IV. Tuning Procedure

Based on the proposed circuit model, a step-by-step deterministic tuning procedure for cascaded coupled resonators filters that eliminates tedious iterative approaches is developed and summarized as follows.

Step 1) The tuning procedure starts with the necessary calibration to determine the proper location of the reference plane for accurate phase measurement.

TABLE I
List of Commonly Used SMA Adapters

Types	*Electrical Length*
Offset Female-to-Female	8.5°
Non-Offset Female-to-Female	1°
Offset Male-to-Male	17.1°
Non-Offset Male-to-Male	3.8°
Male-to-Female	17.3°

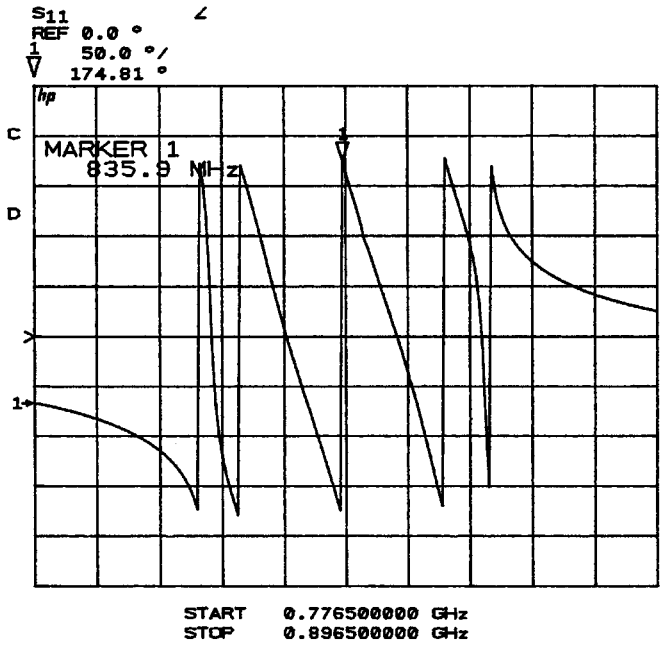

(a)

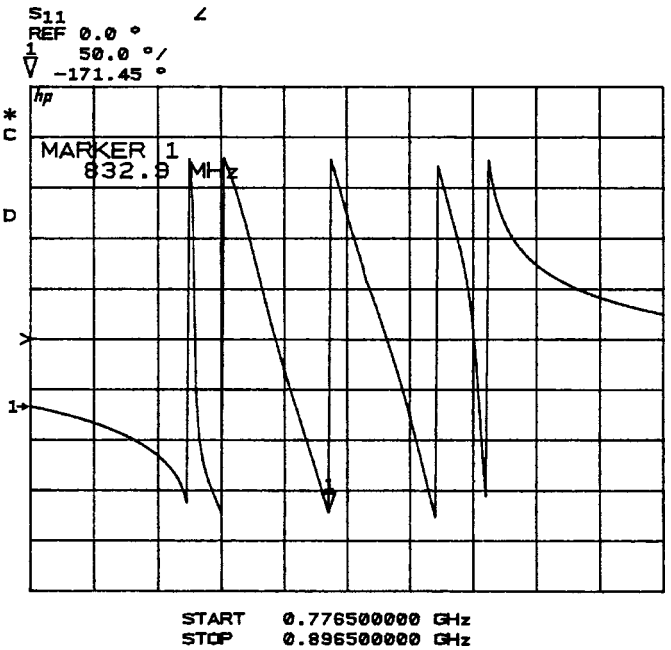

(b)

Fig. 4. Plots of the phase of input reflection coefficient for two different setups for the measurement to remove the loading effect with: (a) $\theta_1 = 17.3°$ inserted and (b) $\theta_2 = 25.6°$ inserted. All five zeros and four poles are clearly shown in both plots indicating the proper choices of θ_1 and θ_2.

TABLE II
SUMMARIZED RESULTS FOR THE THREE MEASUREMENTS FOR THE REMOVAL OF THE LOADING EFFECT TO THE LAST RESONATOR

1st Measurement (θ_0)			2nd Measurement ($\theta_0+\theta_1$)			3rd Measurement ($\theta_0+\theta_2$)		
zeros	poles	f_o's*	zeros	poles	f_o's*	zeros	poles	f_o's*
808.377	810.909	834.583	807.173	808.470	834.602	805.857	806.407	834.699
816.096	825.465	835.656	813.970	823.538	835.699	812.739	822.419	835.723
835.934	846.868	836.428	833.975	844.900	836.559	832.818	843.730	836.788
856.159	863.144	837.104	854.273	861.231	837.092	853.215	860.409	837.102
864.886		836.259	863.888		827.872	863.513		820.595

*: *Extracted resonant frequencies of individual resonators from the recursive relations.*

In practice, the procedure is to insert all the filter tuning screws deep into the cavities so that their resonant frequencies are far from the desired resonant frequencies of the individual cavities (the detuned condition). This condition is observed on the polar display of a network analyzer when the input reflection coefficient appears as a single spot, while the frequency is being swept several times the bandwidth around the desired center frequency. The phase reference plane is then adjusted to achieve the "best" spot on the sweep, which will be used to correspond to the 0° position of the reflection coefficient.

Step 2) The measurement and adjustment of the input and output couplings are then performed. In this step, only the first resonator is brought into resonance, while all the remaining resonators in the network are still in the detuned condition. Following the same procedures as in [8], the input coupling resistance R_1 is determined. Possible adjustment of R_1 to the desired value is performed by changing the iris dimension or probe position, depending on the coupling schemes adapted. The same method is applied for the measurement and adjustment of the output coupling resistance R_n.

Step 3) Terminate the output port with a short circuit and look at the phase of the input reflection coefficient. Bring in all the resonators in the network into resonance. This can be achieved by adjusting the tuning screws until all the zeros and poles are shown on the display of network analyzer.

Step 4) Make the measurement of the above network. Record all the zeros and poles as $\left\{f_{zi}^{(0)};\, f_{pj}^{(0)}\right\}_{i=1,\ldots,n;\, j=1,\ldots,n-1}$. From (5) to (8), extract the inter-resonator couplings and resonant frequencies of each individual resonators $\left\{f_{oi}^{(0)};\, m_{j,j+1}^{(0)}\right\}_{i=1,\ldots,n;\, j=1,\ldots,n-1}$. At this point, the extracted filter parameters $\left\{f_{oi}^{(0)};\, m_{j,j+1}^{(0)}\right\}_{i=1,\ldots,n;\, j=1,\ldots,n-1}$ are expected to be different from the desired ones $\left\{\hat{f}_{oi};\, \hat{m}_{j,j+1}\right\}_{i=1,\ldots,n;\, j=1,\ldots,n-1}$.

Step 5) From $\left\{f_{oi}^{(0)};\, \hat{m}_{12}, m_{23}^{(0)}, \ldots, m_{j,j+1}^{(0)}\right\}_{i=1,\ldots,n;\, j=2,\ldots,n-1}$, synthesize the zeros and poles and record as $\left\{f_{zi}^{(1)};\, f_{pj}^{(1)}\right\}_{i=1,\ldots,n;\, j=1,\ldots,n-1}$. This set of zeros and poles will be used as the criterion for the adjustment of the coupling between resonators 1 and 2. The underlying concept here is that if the zeros and poles are placed to the recorded positions through the adjustment of the corresponding tuning screw, $m_{12}^{(1)}$ will be equal to $\hat{m}_{12}$, which is the desired value.

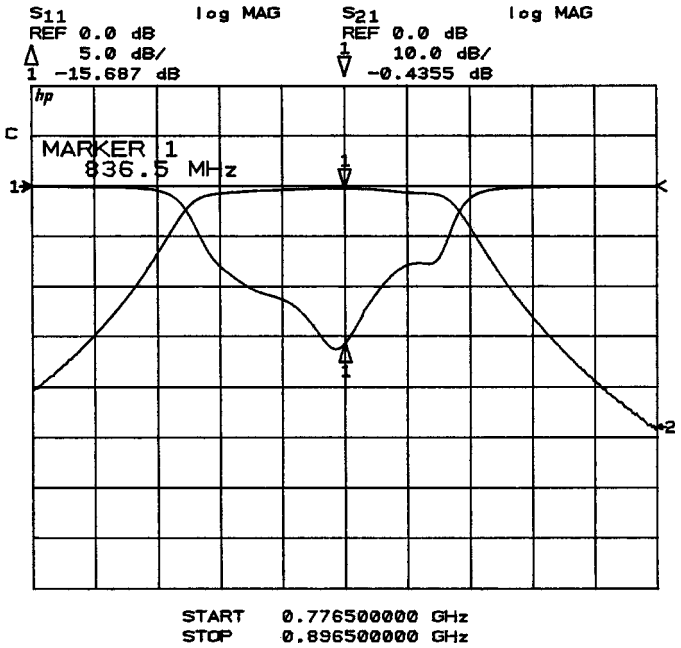

Fig. 5. Filter response after all the five resonators are brought into resonance (i.e., Step 3) before the adjustment of the parameters is made.

Step 6) Repeat Step 5 for all the coupling elements until the $(n-1)$th set of zeros and poles, $\left\{f_{zi}^{(n-1)};\, f_{pj}^{(n-1)}\right\}_{i=1,\ldots,n;\, j=1,\ldots,n-1}$ synthesized from $\left\{f_{oi}^{(0)};\, \hat{m}_{12}, \hat{m}_{23}, \hat{m}_{34}, \ldots, \hat{m}_{n-1,n}\right\}_{i=1,\ldots,n}$ has been recorded.

Step 7) Repeat Steps 5 and 6 for all the resonant frequencies of individual resonators. Starting from $\left\{\hat{f}_{o1}, f_{oi}^{(0)};\, \hat{m}_{j,j+1}\right\}_{i=2,\ldots,n;\, j=1,\ldots,n-1}$, all the zeros and poles are synthesized and recorded until the last, i.e., $(2n-1)$th, set of zeros and poles is synthesized from $\left\{\hat{f}_{o1}, \hat{f}_{o2}, \ldots, \hat{f}_{on};\, \hat{m}_{j,j+1}\right\}_{j=1,\ldots,n-1}$. These $(2n-1)$ sets of zeros and poles will be the criteria for the adjustment of the $(2n-1)$ filter parameters. It might seem lengthy at this point, however, all the steps from Steps 4 to 7 can easily be implemented

$\left\{\hat{f}_{oi}, \hat{m}_{j,j+1}\right\}=$ { 836.500, 836.500, 836.500, 836.500, 835.260; 40.263, 27.881, 27.881, 40.220 }

$\left\{f_{zi}^{(0)}; f_{pj}^{(0)}\right\}=$ { 805.856, 812.739, 832.818, 853.215, 863.512; 806.407, 822.419, 843.730, 860.409 }

$\left\{f_{oi}^{(0)}; m_{j,j+1}^{(0)}\right\}=$ { 834.699, 835.817, 837.132, 838.537, 820.594; 39.905, 27.482, 27.296, 38.073 }

1	f_{o5}	[834.699, 835.817, 837.132, 838.537, 835.260; 39.905, 27.482, 27.296, 38.073]	{809.365, 816.952, 836.070, 855.822, 864.593; 812.427, 825.812, 846.729, 862.660}
2	m_{45}	[834.699, 835.817, 837.132, 838.537, 835.260; 39.905, 27.482, 27.296, 40.220]	{809.092, 816.323, 836.092, 856.309, 865.038; 811.734, 825.542, 847.026, 863.378}
3	f_{o4}	[834.699, 835.817, 837.132, 836.500, 835.260; 39.905, 27.482, 27.296, 40.220]	{808.662, 815.776, 836.091, 855.840, 864.448; 810.877, 825.425, 846.868, 862.472}
4	f_{o1}	[836.500, 835.817, 837.132, 836.500, 835.260; 39.905, 27.482, 27.296, 40.220]	{808.911, 816.219, 836.532, 856.297, 864.658; 810.877, 825.425, 846.868, 862.472}
5	f_{o2}	[836.500, 836.500, 837.132, 836.500, 835.260; 39.905, 27.482, 27.296, 40.220]	{809.075, 816.399, 836.532, 856.464, 864.830; 810.920, 825.731, 847.153, 862.521}
6	f_{o3}	[836.500, 836.500, 836.500, 836.500, 835.260; 39.905, 27.482, 27.296, 40.220]	{808.928, 816.398, 836.205, 856.464, 864.673; 810.779, 825.557, 846.995, 862.361}
7	m_{34}	[836.500, 836.500, 836.500, 836.500, 835.260; 39.905, 27.482, 27.881, 40.220]	{808.786, 816.406, 836.196, 856.469, 864.822; 810.602, 825.628, 846.912, 862.559}
8	m_{23}	[836.500, 836.500, 836.500, 836.500, 835.260; 39.905, 27.881, 27.881, 40.220]	{808.695, 816.400, 836.197, 856.466, 864.926; 810.556, 825.494, 847.044, 862.616}
9	m_{12}	[836.500, 836.500, 836.500, 836.500, 835.260; 40.263, 27.881, 27.881, 40.220]	{808.637, 816.309, 836.196, 856.555, 864.995; 810.556, 825.494, 847.044, 862.616}

Fig. 6. Spreadsheet for the illustration of the tuning steps. The first column indicates the step count. The second column indicates the corresponding filter parameter to be adjusted in the specific step. The numbers in [] (third column) are the filter parameters used to synthesize the zeros and poles (numbers in {}, column 4) to be recorded as the tuning criterion of each step. This table can be generated in seconds by implementing the model on a computer.

on a computer. It takes just seconds to perform all the above computations.

Step 8) The adjustment process begins with m_{12}, the coupling between the first and second resonator. Set the markers on the network analyzer at the corresponding frequencies of zeros and poles $\left\{f_{zi}^{(1)}; f_{pj}^{(1)}\right\}_{i=1,\ldots,n;\, j=1,\ldots,n-1}$. At this point, all the markers should be randomly spaced on the polar display of the network analyzer. Adjust the corresponding tuning screw until the markers "merge" into two clusters on the polar display. The cluster at the far left-hand-side end of the polar display corresponds to the frequencies of zeros, while that at the right-hand side corresponds to poles.

Step 9) The whole procedure ends after repeating Step 8 for $(2n-2)$ more times to finish adjusting the rest of the filter parameters to the desired values.

It is clear that, in general, only $(2n-1)$ tuning steps are required for a filter with n resonators after the input/output couplings have been correctly tuned. This tuning procedure has been proven to be successful both theoretically and experimentally. The practical application of the tuning procedure on a five-pole combline Chebyshev filter will be presented in Section V.

V. Applications

To demonstrate the powerfulness of the proposed model and tuning procedure, a five-pole combline Chebyshev filter with center frequency of 836.5- and 40-MHz bandwidth was used. Fig. 3 shows the theoretical response of the filter. Necessary calibration and accurate determination of reference plane for phase measurement are performed following the procedure outlined in Section IV. Since tapped line realization is used for input/output coupling, the position of the tap is adjusted to achieve the desired coupling. The measured input and output coupling resistances (R_1 and R_n) after adjustment are 1.310 and 1.306, which are both close to the desired value of 1.322.

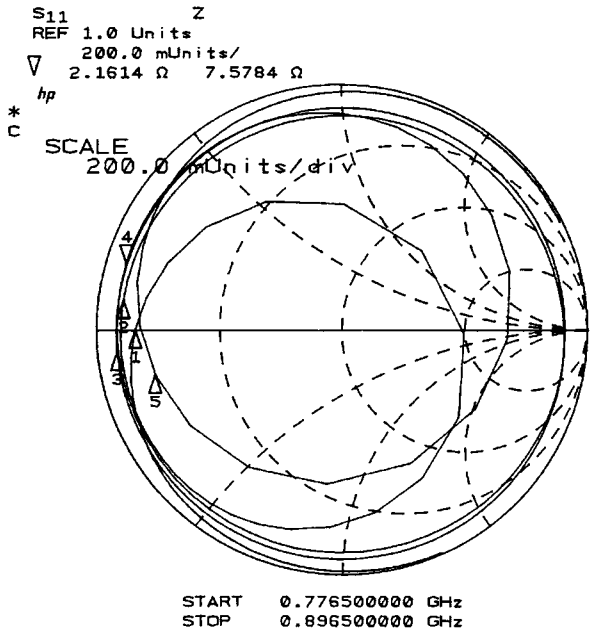

(a)

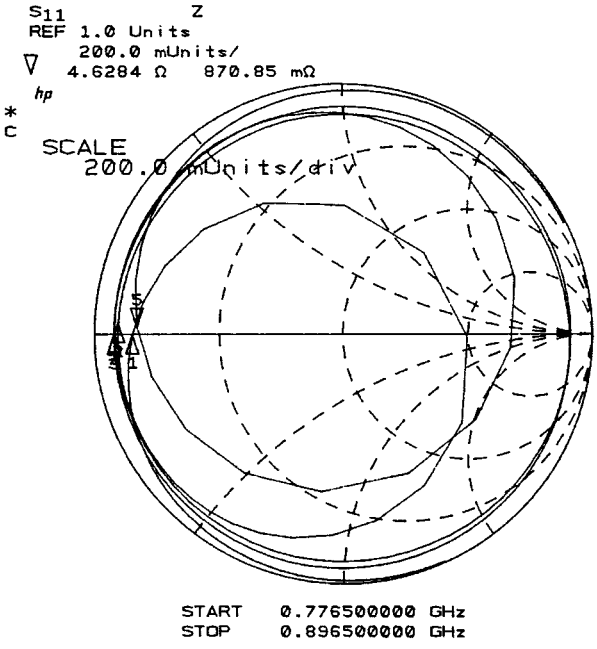

(b)

Fig. 7. Polar displays from the network analyzer: (a) before and (b) after adjustment of the f_{o5} tuning screw. The markers are corresponding frequencies of the zeros. It is observed that all the markers merge into a cluster after tuning.

The method for the removal of the loading effect is then applied. In our measurement setup, 401 frequency points in a frequency span of 120 MHz (a frequency resolution of 0.3 MHz) are used. A linear interpolation technique is adapted for accurate determination of the positions of zeros and poles. It should be noted that higher measurement accuracy may be achieved by taking more frequency points in the same frequency span (which means higher resolution) at the price of longer sweeping time per cycle on the network analyzer. As is addressed before, choices of the two transmission lines θ_1 and θ_2 are important. In practice, various types of the SMA

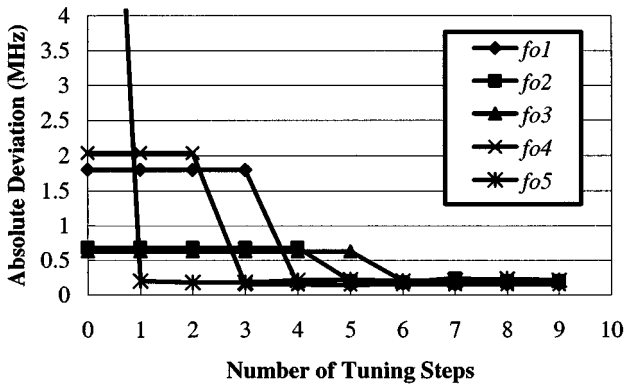

(a)

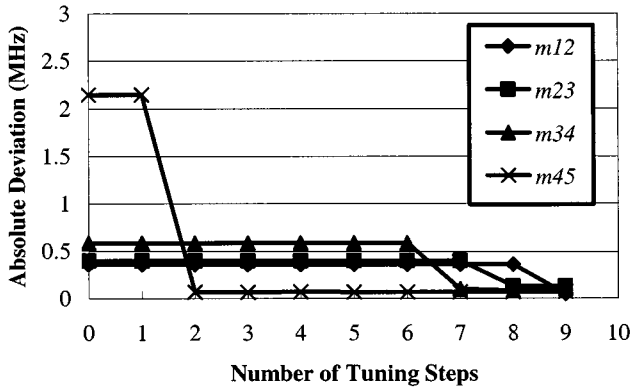

(b)

Fig. 8. Convergence plots of: (a) resonant frequencies of individual resonators and (b) inter-resonator couplings with respect to the number of tuning steps.

adapters are good candidates. Several commonly used SMA adapters are listed in Table I with electrical length measured at the center frequency 836.5 MHz.

In our case, the two lines are chosen to be 17.3° and 25.6°. To check the properness of these choices, plots of the phase of the input reflection coefficients for both cases are shown in Fig. 4. As is observed in both plots, the existence of all five zeros and four poles reveals that both networks are near the optimum approximation to the requirements. The measured zeros and poles for all three measurements are summarized in Table II. With (11)–(13) and the measurement results in Table II, the shift in reference plane θ_0 is solved to be 2.41° at the center frequency. The corresponding frequency adjustment to the last resonator, from (15), is $\Delta f = -1.2$ MHz.

Before changing any tuning screws, all the computations required in Steps 4–7 of the tuning procedure is performed by a computer. To further highlight the efficiency of the proposed technique, the filter response after all the resonators are brought into resonance (i.e., Step 3) is checked and shown in Fig. 5 before we proceed with the adjustment of each tuning screw. Fig. 6 is a spreadsheet that records the nine sets of zeros and poles as criteria for tuning with the desired filter parameters included. The sequence for adjusting the filter parameters outlined in the tuning procedure is for the convenience of illustration only. In practice, one can pick any sequence to perform the tuning process. The underlying fact is that, once a parameter is adjusted, the impact from the adjustment of other

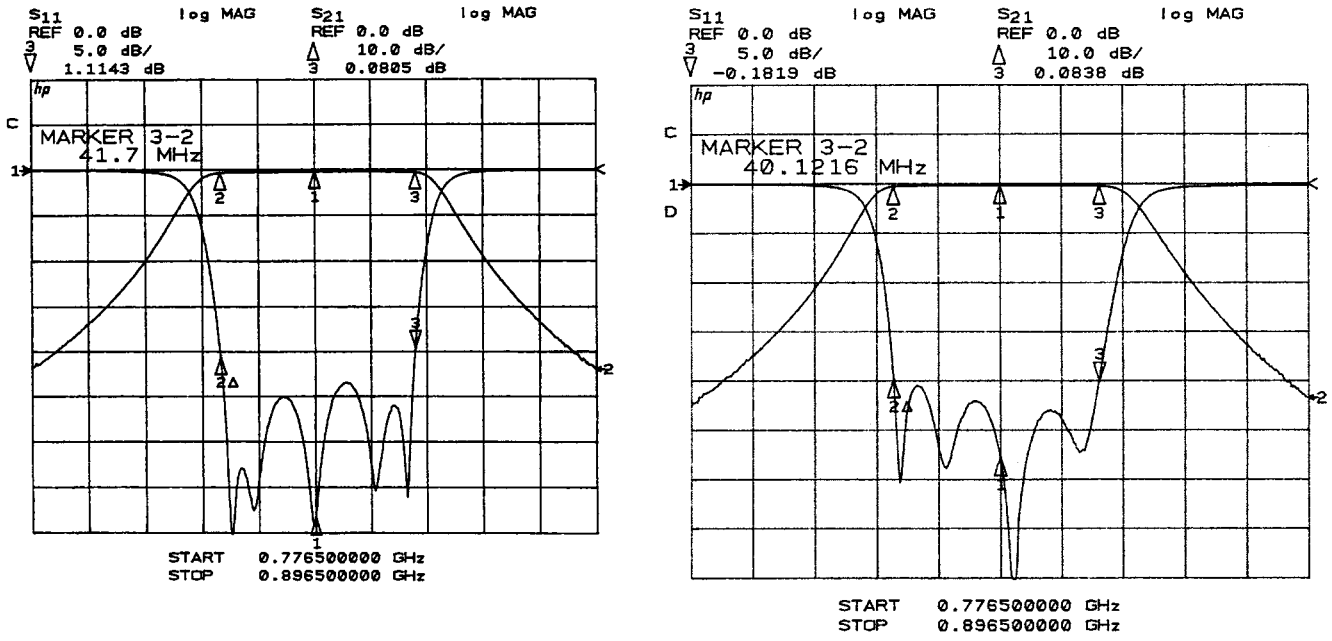

(a) (b)

Fig. 9. (a) Final response after only nine tuning steps performed. (b) Response from [13] without the removal of the loading effect to the last resonator.

TABLE III
MEASURED ZEROS/POLES AND EXTRACTED FILTER PARAMETERS AFTER TUNING

Frequency (MHz)			Coupling (MHz)		
	Measured	*Required*		*Measured*	*Required*
f_{01}	836.320	836.500	m_{12}	40.210	40.263
f_{02}	836.711	836.500	m_{23}	27.751	27.881
f_{03}	836.403	836.500	m_{34}	28.120	27.881
f_{04}	836.352	836.500	m_{45}	40.152	40.220
f_{05}	835.012	835.260			
Zeros (MHz)			**Poles (MHz)**		
	Measured	*Required*		*Measured*	*Required*
f_{z1}	808.563	808.637	f_{p1}	810.392	810.555
f_{z2}	816.258	816.309	f_{p2}	825.578	825.494
f_{z3}	836.049	836.196	f_{p3}	846.962	847.044
f_{z4}	856.435	856.554	f_{p4}	862.537	862.616
f_{z5}	864.945	864.995			

parameters will be secondary. Thus, the change in the adjusted parameter will be small so that there is not much influence on the final filter response. In our case, we start with f_{o5}, which is found to have the maximum deviation from desired value by comparing $\left\{f_{oi}^{(0)}; m_{j,j+1}^{(0)}\right\}_{i=1,\ldots,n;\, j=1,\ldots,n-1}$ with $\left\{\hat{f}_{oi}; \hat{m}_{j,j+1}\right\}_{i=1,\ldots,n;\, j=1,\ldots,n-1}$.

Fig. 7 shows the polar display from network analyzer before [see Fig. 7(a)] and after [see Fig. 7(b)] the adjustment of the corresponding f_{o5} tuning screw. Limited by the network analyzer, only the markers corresponding to the frequencies of zeros are shown. Note that the difference in the radius of the circles on the polar plot is caused by the loss of each individual resonator. The filter parameters are computed and compared to the desired values after each adjustment. Fig. 8 summarizes the convergence of each parameter with respect to the number of tuning steps. It is clearly observed that all the parameters converge to their desired values after nine tuning steps.

Fig. 9(a) shows the final filter response after only nine tuning steps are performed. The response from a previously published paper [13] [see Fig. 9(b)] without the removal of the loading effect to the last resonator is also included for comparison. The measured zeros and poles and extracted filter parameters after tuning [see Fig. 9(a)] together with the desired values are tabulated in Table III.

VI. CONCLUSIONS

A general model for determination of individual resonant frequencies and coupling coefficients of a system with cas-

caded coupled resonators based on the knowledge of the zeros and poles of the network has been developed. The model is very useful for effective tuning and diagnosis of cascaded coupled resonators filters and can also be used in conjunction with full-wave simulations to simulate the couplings and resonant frequencies for networks consisting of nonidentical resonators.

The importance of the loading effect to the last resonator has been pointed out in this paper for the first time. This loading effect can be effectively removed by the proposed systematic method. A new tuning procedure for cascaded coupled resonator filters has also been proposed and tested experimentally. The deterministic and noniterative characteristic of the tuning procedure makes the possibility of fully automatic filter tuning promising.

REFERENCES

[1] M. Dishal, "Alignment and adjustment of synchronously tuned multiple-resonator circuit filters," *Proc. IRE*, vol. 39, pp. 1448–1455, Nov. 1951.

[2] A. E. Atia and A. E. Williams, "Measurements of intercavity couplings," *IEEE Trans. Microwave Theory Tech.*, vol. MTT-23, pp. 519–522, June 1975.

[3] H. L. Thal, "Computer-aided filter alignment and diagnosis," *IEEE Trans. Microwave Theory Tech.*, vol. MTT-26, pp. 958–963, Dec. 1978.

[4] G. Muller, "On computer-aided tuning of microwave filters," in *Proc. Int. Symp. Circuits Syst.*, 1976, pp. 201–211.

[5] M. H. Chen, "Short-circuit tuning method for single terminated filters," *IEEE Trans. Microwave Theory Tech.*, vol. MTT-25, pp. 1032–1036, Dec. 1977.

[6] H. W. Yao, K. A. Zaki, A. E. Atia, and R. Hershtig, "Full wave modeling of conducting posts in rectangular waveguide and its applications to slot coupled combline filters," *IEEE Trans. Microwave Theory Tech.*, vol. 43, pp. 2824–2830, Dec. 1995.

[7] L. Accatino, "Computer-aided tuning of microwave filters," in *IEEE MTT-S Int. Microwave Symp. Dig.*, 1986, pp. 249–252.

[8] A. E. Williams, R. G. Egri, and R. R. Johnson, "Automatic measurement of filter coupling parameters," in *IEEE MTT-S Int. Microwave Symp. Dig.*, 1983, pp. 418–420.

[9] J. Dunsmore, "Tuning band pass filters in the time domain," in *IEEE MTT-S Int. Microwave Symp. Dig.*, 1999, pp. 1351–1354.

[10] C. Wang, H. W. Yao, K. A. Zaki, and R. Mansour, "Mixed modes cylindrical planar dielectric resonator filters with rectangular enclosure," *IEEE Trans. Microwave Theory Tech.*, vol. 43, pp. 2817–2823, Dec. 1995.

[11] N. I. Achieser, *Theory of Approximation*. New York: Frederick Unger, 1956.

[12] A. E. Atia, A. E. Williams, and R. W. Newcomb, "Narrowband multiple-coupled cavity synthesis," *IEEE Trans. Circuits Syst.*, vol. CAS-21, pp. 649–655, 1974.

[13] A. E. Atia and H. W. Yao, "Tuning and measurement of couplings and resonant frequencies for cascaded resonators," in *IEEE MTT-S Int. Microwave Symp. Dig.*, 2000, pp. 1637–1640.

Heng-Tung Hsu (S'98) received the B.S. and M.S. degrees in electronics engineering from the National Chiao Tung University, Hsinchu, Taiwan, R.O.C., in 1993 and 1995, respectively, and is currently working toward the Ph.D. degree in electrical and computer engineering at the University of Maryland at College Park.

Hui-Wen Yao (S'92–M'95–SM'97) received the B.S. and M.S. degrees from the Beijing Institute of Technology, Beijing, China, in 1983 and 1986, respectively, and the Ph.D. degree from the University of Maryland at College Park in 1995, all in electrical engineering.

From 1986 to 1991, he was a Lecturer with the Department of Electrical Engineering, Beijing Institute of Technology, where his research dealt mainly with electromagnetic radiation, scattering, and antenna design. From 1992 to 1995, he was a Research Assistant in the Department of Electrical Engineering, University of Maryland at College Park, where he was involved with the analysis, modeling, and design of microwave and millimeter-wave devices and circuits. In 1995, he joined CTA Inc. Since 1997, he has been with the Orbital Sciences Corporation, Germantown, MD, where he is responsible for satellite communications systems. He has authored or co-authored 50 technical papers.

Dr. Yao is on the Editorial Board of the IEEE TRANSACTIONS ON MICROWAVE THEORY AND TECHNIQUES. He was the recipient of the 1998 Outstanding Technical Achievement Award presented by the Orbital Sciences Corporation.

Kawthar A. Zaki (SM'85–F'91) received the B.S. degree (with honors) from Ain Shams University, Cairo, Egypt, in 1962, and the M.S. and Ph.D. degrees from the University of California at Berkeley, in 1966 and 1969, respectively, all in electrical engineering.

From 1962 to 1964, she was a Lecturer in the Department of Electrical Engineering, Ain Shams University. From 1965 to 1969, she was a Research Assistant in the Electronics Research Laboratory, University of California at Berkeley. In 1970, she joined the Electrical Engineering Department, University of Maryland at College Park, where she is currently a Professor of electrical engineering. Her research interests are in the areas of electromagnetics, microwave circuits, simulation, optimization, and computer-aided design of advanced microwave and millimeter-wave systems and devices. She has authored or co–authored over 200 publications. She holds five patents on filters and dielectric resonators.

Prof. Zaki was the recipient of several academic honors and awards for teaching, research, and inventions.

Ali E. Atia (S'67–M'69–SM'78–F'87) received the B.S. degree from Ain Shams University, Cairo, Egypt, in 1962, and the M.S. and Ph.D. degrees in electrical engineering from the University of California at Berkeley, in 1966 and 1969, respectively.

He is currently the President and with the Space Systems Group, Orbital Sciences Corporation, Germantown, MD, where he is responsible for the communications business area, which builds communications and broadcasting satellites. In 1969, he joined COMSAT Laboratories, where he participated in research and development of a broad range of advanced microwave technologies for communication satellite transponders and antennas. He designed, developed, and implemented microwave flight hardware (mixers, filters, multiplexers, amplifiers, switches, antennas, etc.) for several satellite programs covering L- through the Ka- frequency bands. While with COMSAT Laboratories, he and his coworkers invented the dual-mode waveguide multiple coupled cavity filters, which has become the industry standard for input and output multiplexers in communication satellites, as well as other challenging filtering requirements. He has participated in and directed system development and software activities for several satellite programs and ground stations projects for customers including INTELSAT, INMARSAT, ARABSAT, and others. He has held several technical and management positions at COMSAT, the most recent of which was Vice President and Chief Engineer for the COMSAT Technology Services and COMSAT Systems Division. He has authored or co-authored over 100 refereed technical papers and presentations in IEEE publications and various national and international conferences and symposia. He holds five patents in the areas of microwave filters and receivers.

Dr. Atia is a Fellow of the American Institute of Aeronautics and Astronautics (AIAA). He is a member of Sigma Xi.